ORIGINAL PAPER

Rapid direct analysis in real time (DART) mass spectrometric detection of juvenile hormone III and its terpene precursors

Arti T. Navare · Jaime G. Mayoral · Marcela Nouzova ·
Fernando G. Noriega · Facundo M. Fernández

Abstract Direct analysis in real time (DART) is a plasma-based ambient ionization technique that enables rapid ionization of small molecules with high sample throughput. In this work, DART was coupled to an orthogonal (oa) time-of-flight (TOF) mass spectrometer and the system was optimized for analyzing a vital hormonal regulator in insects, juvenile hormone (JH) III and its terpene precursors, namely, farnesol, farnesoic acid, and methyl farnesoate. Optimization experiments were planned using design of experiments (DOE) full factorial models to identify the most significant DART variables contributing to JH III analysis sensitivity by DART-TOF mass spectrometry (MS). The optimized DART-TOF MS method had femto-mole to sub-picomole detection limits for terpene standards, along with mass accuracies below 5 ppm. Finally, the possibility of distinguishing between two farnesol isomers by in-source-collision-induced dissociation (CID) in the first differentially pumped region of the oaTOF mass spectrometer was investigated. DART-MS enabled high-throughput, sensitive analysis with acquisition times ranging from 30 s to a minute. To the best of our knowledge, this is the first report on the application of DART-MS to the detection and identification of volatile or semi-volatile insect terpenoids, and on the use of DOE approaches to optimize DART-MS analytical procedures.

Keywords Mass spectrometry/ICP-MS · Biological samples · Bioanalytical methods

Introduction

Juvenile hormone (JH) plays key roles regulating development and reproduction in insects [1]. Reproducible and sensitive detection of JH and related chemical species is crucial for better understanding insect endocrinology and for developing safer insecticides that target JH as a way of controlling insects vector of diseases or agricultural pests [2, 3]. JH is synthesized and released from the *corpora allata*, a pair of endocrine glands with neural connections to the brain [4]. The early steps of JH III biosynthesis follow the mevalonate pathway, with the formation of five-carbon (5C) isoprenoid units from acetate via mevalonic acid, with the subsequent head to tail condensation of three 5C units to form farnesyl diphosphate (FPP) [5]. In the late steps, FPP is hydrolyzed by a pyrophosphatase [6] to form farnesol followed by successive oxidations to farnesal and farnesoic acid (FA) by an alcohol dehydrogenase [7] and an aldehyde dehydrogenase [8], respectively. In most insects, the last two biosynthetic steps involve methylation of FA by an *O-S*-adenosylmethinine-dependent methyltransferase [9] to form methyl farnesoate (MF) that is subsequently epoxidated to JH III by a P450 monooxygenase [10]. The amount of these compounds in small insects is in the femtomole to picomole range, which makes it challenging to detect them by most typical analytical techniques [11–16].

A. T. Navare · F. M. Fernández (✉)
School of Chemistry and Biochemistry,
Georgia Institute of Technology,
901 Atlantic Dr. NW,
Atlanta, GA 30332-0400, USA
e-mail: facundo.fernandez@chemistry.gatech.edu

J. G. Mayoral · M. Nouzova · F. G. Noriega
Department of Biological Sciences,
Florida International University,
Miami, FL 33199, USA

The most commonly used analytical methods for identification and detection of JH III and its precursors include NMR, IR, and gas chromatography (GC)–mass spectrometry (MS) [17, 18], the latter two being the tools of choice for distinguishing between different farnesol isomers [19]. Due to the volatile nature of JH III and its precursors, electron ionization (EI) or chemical ionization (CI) are commonly used following GC separation, with the main drawback of EI being the extensive fragmentation observed [19]. Although fragment ions are useful for identification purposes in low resolving-power-MS experiments, unwanted fragmentation also complicates the mass spectrum and reduces sensitivity. In addition, GC separations are time consuming, with memory effects and stationary phase bleeding being some of the most common practical issues. Such limitations motivated us to investigate the application of ambient ionization techniques for direct mass spectrometric analysis of this family of related compounds.

Direct analysis in real time (DART) is one of the more popular ambient pressure ionization methods. It allows for rapid MS analysis of small molecules without chromatography and with minimal sample preparation [20, 21]. The DART ionization process starts by generating excited metastable gaseous species of nitrogen (N_2) or atomic helium (He) in an enclosed chamber containing a point-to-plane glow discharge. The metastable species are then heated in the ion source and directed towards the sample held in the gap between the DART source outlet and the mass spectrometer inlet. In positive ion mode, the metastables interact with ambient gases by Penning ionization [22] generating a series of rapid gas-phase chemical reactions that produce protonated water clusters. These clusters ionize the thermally desorbed analyte by proton transfer reactions [20]. The versatility of DART in ionizing a wide range of chemicals without the need of extensive sample preparation has motivated MS practitioners to apply the technique in various fields such as forensic drug discovery [20, 23, 24], reaction monitoring [24], counterfeit drug detection [25–27], contaminated pet food analysis [28], detection of restricted phthalic acid esters in toys [29], fragrance analysis [30], bacterial strain classification [31], and rapid human serum fingerprinting [32].

We have previously reported the use of DART-orthogonal (oa) time-of-flight (TOF) MS for confirming the biochemical role of an $NADP^+$-dependent farnesol-dehydrogenase enzyme in *Aedes aegypti* [7]. In this follow-up work, we present an extensive full factorial design optimization process for further improving DART-MS analysis of farnesol, FA, MF, and JH III at lower concentrations, also shedding more light on the physico-chemical processes involved in ion generation. The utility of the optimized DART-MS approach was further evaluated for distinguishing between (2Z,6Z)- and (2E,6E)-farnesol isomers via in-source collision-induced dissociation (CID).

Experimental

Reagents and chemicals

HPLC-grade methanol was purchased from EMD Chemicals Inc. (Gibbstown, NJ, USA). DIP-it sampler glass capillaries were purchased from IonSense Inc. (Danvers, MA, USA). PEEK tubing (O.D. 360 μm, I.D. 50 μm) was obtained from Health and Science (Oak Harbor, WA, U.S.A.). Juvenile hormone (JH) III, (2E,6E)-farnesol and poly (ethylene glycol) (PEG) 600 were obtained from Sigma-Aldrich (St. Louis, MO, USA). (2Z,6Z)-farnesol, MF, and (E,E)-FA were purchased from Echelon (Salt Lake City, UT). The purity of all chemicals was higher than 85% as confirmed using HPLC or gas chromatography (GC).

Sample preparation

All standard solutions were prepared in HPLC-grade methanol. For optimization studies, a 4 mM (2E,6E)-farnesol working solution was prepared by diluting 4 M neat farnesol. Serial dilutions of standard (2E,6E)-farnesol, FA, MF, and JH III containing 0.1–5 pmol/μL were prepared for limit of detection (LOD) studies. For in-source CID experiments, 100 μg of (2Z,6Z)-farnesol and (2E,6E)-farnesol were dissolved in methanol to prepare 4 mM stock solutions, which were subsequently diluted to 2 μM prior to experiments.

DART-oaTOF instrumentation

A DART-100 ion source from IonSense Inc. (Saugus, MA, USA) was interfaced to an oaTOF mass spectrometer (AccuTOF) from JEOL USA, Inc. (Peabody, MA, USA). A detailed description of the commercial DART-AccuTOF setup can be found elsewhere [33]. The distance between the DART source exit and the oaTOF cone inlet was 12 mm. The DART discharge needle voltage of +3,600 V and perforated electrode voltage of +150 V were kept constant for all experiments. During optimization studies, the DART exit grid voltage was varied between 50 and 200 V, while the DART gas temperature and flow rate ranged from 50–200 °C, and 0.55–2 L/min, respectively.

The oaTOF mass spectrometer settings were as follows: orifice 1 temperature=80 °C, orifice 1 voltage=+20 V, orifice 2=+5 V, ring electrode=5 V, ion guide peaks voltage=300 V, and detector voltage=−2750 V. For optimization studies and in-source CID experiments, each total ion chronogram (TIC) was acquired for 0.5 min. For

LOD experiments, five replicates of each standard were collected within 2 min. The data were processed by first creating extracted ion chronograms with an m/z interval of ±0.1 which were then centroided and calibrated using a PEG 600 mass spectrum acquired during the same set of experiments.

DART-oaTOF sample introduction method

Two sample introduction methods, named "manual sample injection", and "continuous sample infusion" were tested and used alternatively during the various studies. In the manual sample injection method, 2 μL of a given working solution were pipette-deposited on the tip of the DIP-it sampler, which was secured by a home-built sampling arm at a fixed vertical position (Electronic supplementary material (ESM), Fig. S1a). During each sample introduction event, the sampling arm was rapidly lowered so that its tip came in contact with the He stream from the DART ion source outlet, producing a transient signal.

In the continuous sample infusion method, the working solution was flowed at 0.55 L/min through a piece of PEEK tubing (360 μm O.D., 50 μM I.D.). One end of the PEEK tube was connected to a syringe pump delivering the fluid, and the other end was permanently positioned into the He gas stream with the aid of an open-ended DIP-it sampler capillary (ESM Fig. S1b). Manual sample injection was implemented for analyzing oxidized terpene alcohol products and for performing LOD studies where high-throughput analysis was desired. Continuous sample infusion was the method of choice for in-source CID analysis of farnesol isomers, and for performing optimization studies where higher reproducibility was needed to statistically weigh the effects of the various experimental factors.

Design of experiments optimization

DOE ++ (Reliasoft Corp., Tucson, AZ, USA) was used to generate a randomized list of experiments to identify factors that significantly affect DART sensitivity. The investigated factors were He gas temperature (factor A), gas flow rate (factor B), and exit grid voltage (factor C). Each of these factors was assigned four levels which were as follows: factor A=50 °C, 100 °C, 150 °C, and 200 °C; factor B= 0.55 L/min, 1.0 L/min, 1.5 L/min, and 2.0 L/min; factor C: 50 V, 100 V, 150 V, and 200 V. Based on these settings, the general full factorial model consisted of 64 unique level combinations for which five replicates were performed, resulting in a total of 320 runs. For each run, the absolute signal intensity of the $[M–H_2O+H]^+$ farnesol ion at m/z 205.1955 was measured. The data was subject to analysis of variance (ANOVA) by means of the DOE++ software. Following the full factorial design, a response surface

methodology design was implemented to generate 39 individual runs to fine tune the optimal settings for the most significant DART factors.

Limit of detection experiments

All LOD experiments were performed using the optimized DART-oaTOF method. Two microliters of standard farnesol, FA, MF, or JH III solutions were spotted on the DIP-it sampler and analyzed using the manual sample injection method, as described previously. Each run was comprised of five replicates.

In-source CID MS experiments

The (2Z,6Z)- and (2E,6E)-farnesol isomers were subject to in-source CID at various orifice 1 fragmentation voltages (20–80 V). Breakdown plots of fragment ions commonly observed in the in-source CID mass spectra of both isomers were plotted and their fragmentation profiles compared.
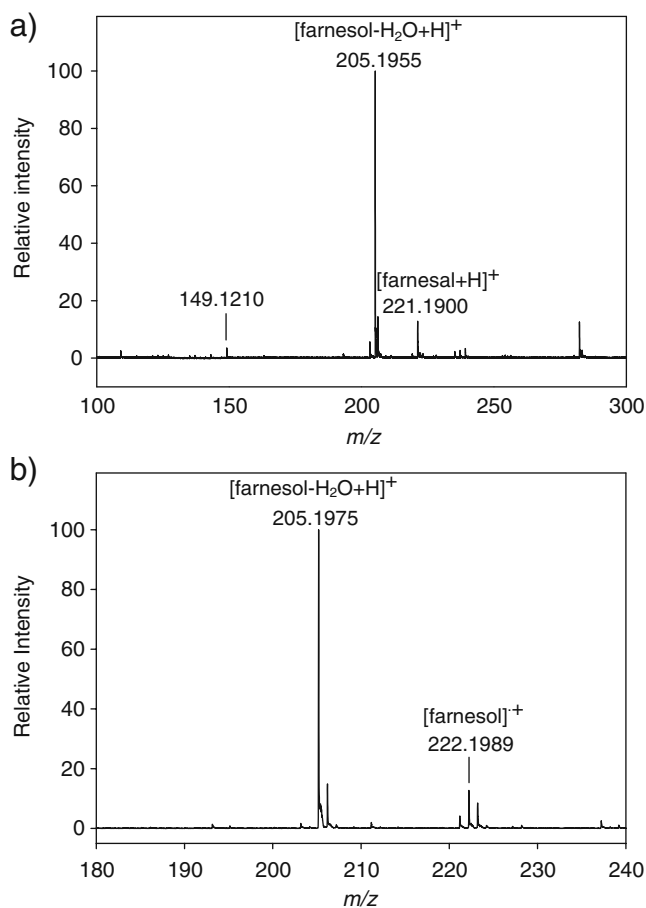
Fig. 1 Typical DART-oaTOF mass spectra of 4 mM farnesol standard solution obtained using **a** a continuous sample infusion method and **b** a manual sample injection method (2b)

Table 1 Analysis of variance (ANOVA) table showing significant DART variables (in italics) affecting DART-oaTOF sensitivity

Source of variation	Degrees of freedom	Sum of squares (partial)	Mean squares (partial)	F ratio	P value
Model	63	7.97E+09	1.27E+08	170.0364	*2.64E−177*
A: gas temperature	3	7.28E+09	2.43E+09	3261.3299	*1.36E−203*
B: gas flow rate	3	5.92E+08	1.97E+08	265.2302	*3.16E−78*
C: grid voltage	3	7.16E+05	2.39E+05	0.3207	0.8104
AB	9	5.40E+07	6.00E+06	8.0615	*1.63E−10*
AC	9	8.82E+06	9.80E+05	1.316	0.2287
BC	9	9.32E+06	1.04E+06	1.3906	0.1925
ABC	27	2.59E+07	9.58E+05	1.2867	0.1621
Residual	256	1.91E+08	7.44E+05		
Pure error	256	1.91E+08	7.44E+05		
Total	319	8.16E+09			

Default P value=0.1. AB indicates the interaction between gas temperature and gas flow rate

Results and discussion

As with any ambient ionization techniques, the sensitivity of DART is a function of the ion yield and ion transmission efficiency from the ambient pressure region into the vacuum regions of the mass spectrometer. Various factors including sample ionization, DART exit to mass spectrometer inlet distance, He gas flow rate, gas temperature, and DART exit grid voltage affect ion transmission in DART [34].

Typical DART-oaTOF mass spectra of the farnesol solution used for optimization purposes showed a base peak at m/z 205.1955 corresponding to the [farnesol–H_2O+ $H]^+$ as shown in the Fig. 1a. The farnesol $[M]^{•+}$ molecular ion at m/z 222.1989 (theoretical mass, 222.1983; mass accuracy, 2.41 ppm) in addition to the protonated farnesol ion peak (Fig. 1b) was observed when manual sample injection was used. The presence of this molecular ion was attributed to a direct Penning ionization process [22]. In this type of a reaction, long-lived He metastables (He*, 2^3S, ionization energy 19.8 eV) react directly with an analyte molecule (M) whose ionization energy is below 19.8 eV, releasing an electron (e$^-$) as shown below (reaction 1)

$$\text{He}^*_{(g)} + \text{M}_{(g)} \rightarrow \text{M}^{•+}_{(g)} + \text{e}^- \quad (1)$$
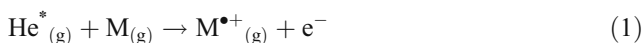
It is likely that the first ionization potential of farnesol is lower than 19.8 eV, as for other common small organic molecules [35–37], facilitating this type of reaction. Another plausible DART molecular ion formation pathway was recently suggested by Cody [38] in which He* atoms first react with ambient O_2 to form $O_2^{•+}$ ions which subsequently react with the analyte (M) to generate $M^{•+}$ in a charge exchange reaction (reactions 2 and 3).

$$\text{He}^* + \text{O}_2 \rightarrow \text{O}_2^{•+} + \text{e}^- + \text{He} \quad (2)$$

$$\text{O}_2^{•+} + \text{M}_{(g)} \rightarrow \text{M}^{•+} + \text{O}_2 \quad (3)$$

It has been reported that certain DART parameters favor molecular ion formation by Penning ionization or charge transfer pathways over the more commonly observed protonated ions. Distances of up to 15 mm between the
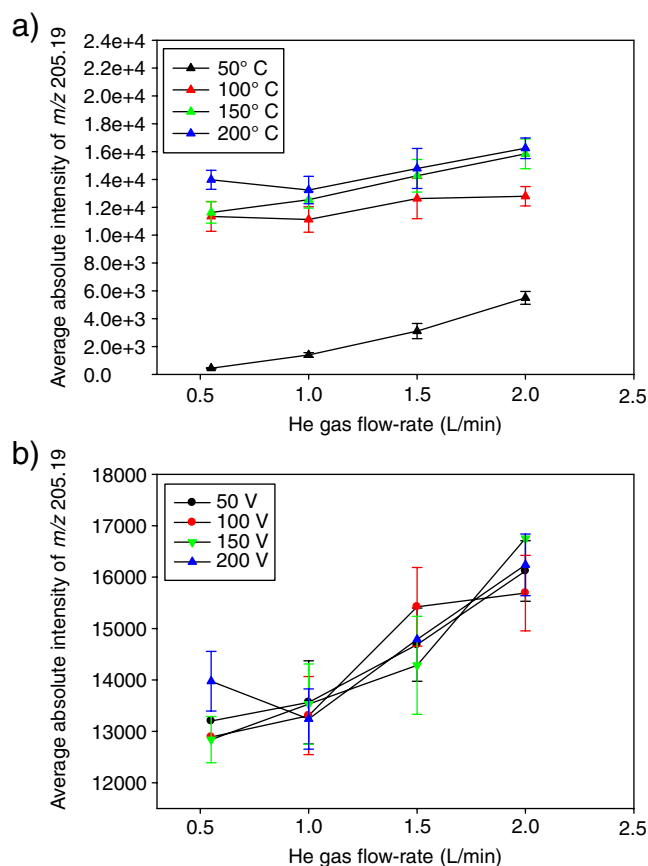

Fig. 2 Determination of the significant DART variable using design of experiments (DOE). Interaction plots showing absolute intensity of m/z 205.1955 as a function of helium gas flow rates at **a** various gas temperatures and at a constant grid voltage of 200 V, and at **b** various grid voltages at and at a constant gas temperature of 200 °C

DART ion source nozzle and the mass spectrometer inlet, exit grid voltages of about 650 V, and placing the sample closer to the DART exit are known to favor $M^{+\cdot}$ ion formation. In the present DART-oaTOF setup, the sample was placed equidistant to the DART exit and the mass spectrometer inlet, while the grid voltage was below 250 V, and the DART exit to MS entrance distance was 12 mm, which explains the observed predominance of protonated analyte species. Cody [38] also suggested that the use of a glass sampling probe, such as the DIP-it sampler used in the present study may

Fig. 3 DART-oaTOF mass spectra of **a** 0.1 pmol/μL of farnesol, 4 pmol/μL of **b** farnesoic acid (*FA*), and **c** methyl farnesoate (*MF*) respectively, and **d** 1 pmol/μL of juvenile hormone (*JH*) III. The molecular structures of the compounds and the theoretical mass values of their protonated ions are shown next to their respective DART-oaTOF mass spectra
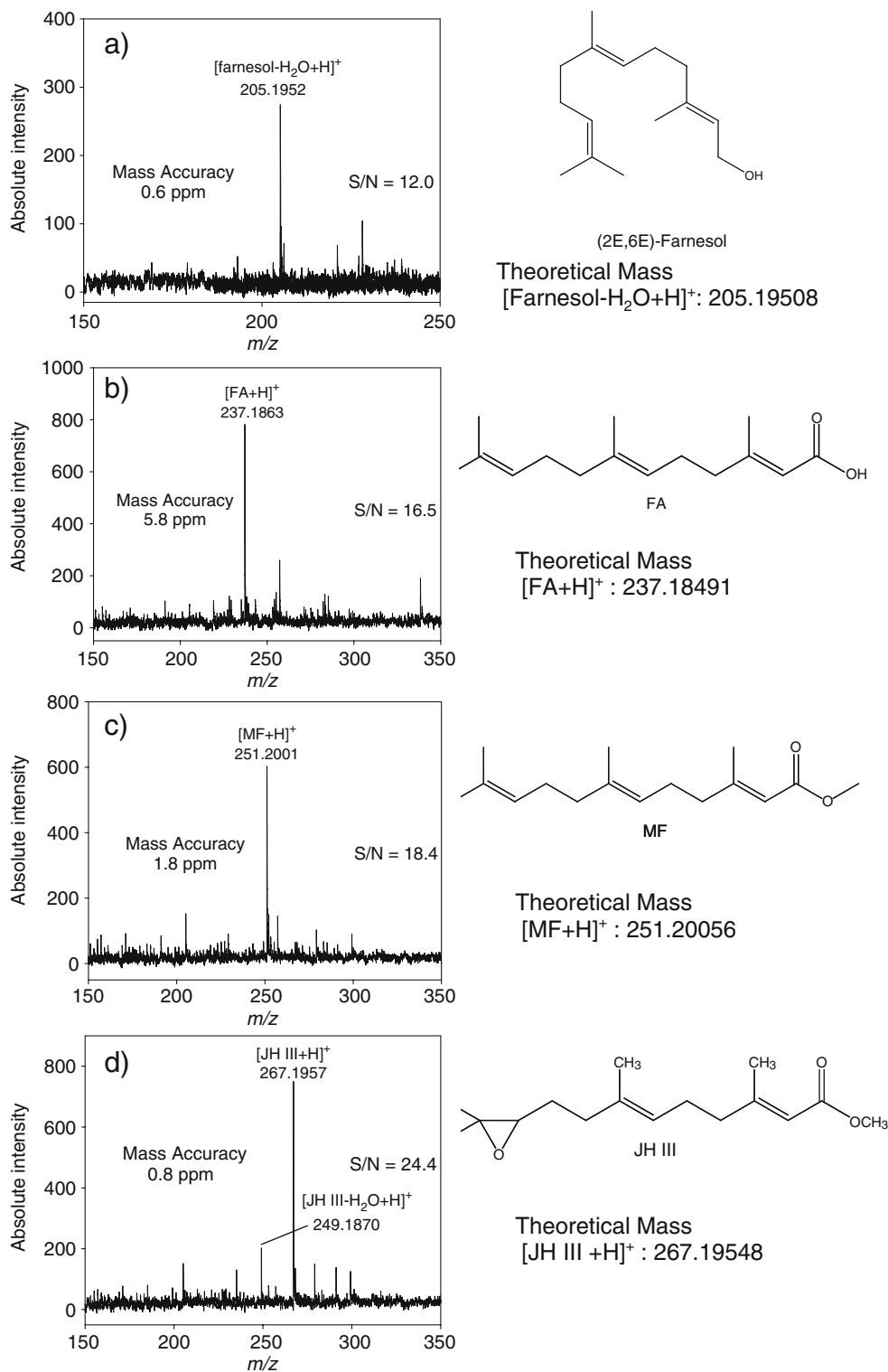
favor molecular ion formation by reducing the relative abundance of NO^+, and increasing the abundance of $O_2{}^{+}$ species under ambient conditions. These observations suggest that the DART-MS conditions can be manipulated to generate specific types of ions in order to analyze polar and nonpolar compounds alike. Additionally, the presence of a molecular ion can be used as an additional diagnostic tool for identification of a compound by DART-MS.

DOE optimization of DART-oaTOF method

Initial optimization experiments performed using the manual sample injection method suffered from large variations in the signal intensities, with percent coefficient of variance (CV) ranging from 20–60% (ESM Fig. S2a), probably due to the volatility of the analytes investigated here. In order to circumvent this problem and to maximize confidence in the design of experiments (DOE) optimization results, a new sample introduction method referred to as "continuous sample infusion" was developed. A comparison of the TICs obtained using both methods clearly showed that in the absence of an autosampler the manual sample injection reproducibility was low (ESM Fig. S2a), whereas the continuous sample infusion method showed a more steady and reproducible signal with percent CV between 5% and 15% (ESM Fig. S2b).

The ANOVA results from the DOE optimization study are shown in Table 1, with the significance of each factor shown by the corresponding P values. These results suggested that He gas temperature (A factor; P value, 1.36×10^{-203}) was the most significant factor, followed by gas flow rate (B factor; P value, 3.16×10^{-78}), and the interaction of the latter two factors (A:B; P value, 1.63×10^{-10}). The DART grid voltage (C factor; P value, 0.8105) was not found significant in the interval tested.

A plot of the [farnesol–H_2O+H]$^+$ signal intensity at various gas flow rates and temperatures, and constant grid voltage (200 V) confirmed the DOE findings, showing that higher gas temperatures and flow rates enhanced sensitivity (Fig. 2a). At elevated gas temperatures, the analyte evaporation rate increases with a concomitant increase in the ion yield. Higher gas flow rates should be beneficial in terms of more efficient ion transport before diffusional losses become predominant. The effect of DART exit grid voltage on the signal intensity was not significant (Fig. 2b). In early DART work, the stated function of the grid voltage was to prevent ion–ion recombination [20], however it appeared as if the weak extraction electric field created by this electrode across the gap between source exit and orifice 1 of oaTOF, also improved transmission under some circumstances. For example, a small increase in signal was observed when varying the grid potential from 50–200 V at low flow rates. However, the ion transmission efficiency improvement caused by carrier gas flow rate increase superseded the ion transmission enhancement caused by this weak electric field as seen in Fig. 2b.

DOE studies indicated that the optimal response was obtained with the following settings: DART gas temperature= between 150 and 200 °C, gas flow rate=2 L/min, and exit grid=between 150 and 200 V. Further optimization of these variables via response surface methodology using a Box–Behnken model concluded that the following optimum settings should be chosen: He gas temperature=200 °C, gas flow rate=2 L/min, and exit grid voltage=180 V.

Fig. 4 DART-oaTOF in-source collision-induced dissociation (CID) mass spectra obtained at orifice voltages of a,c 40 V and b,d 60 V for ZZ- and EE-isomer of farnesol. Insets in a and b show molecular structures of the two farnesol isomers
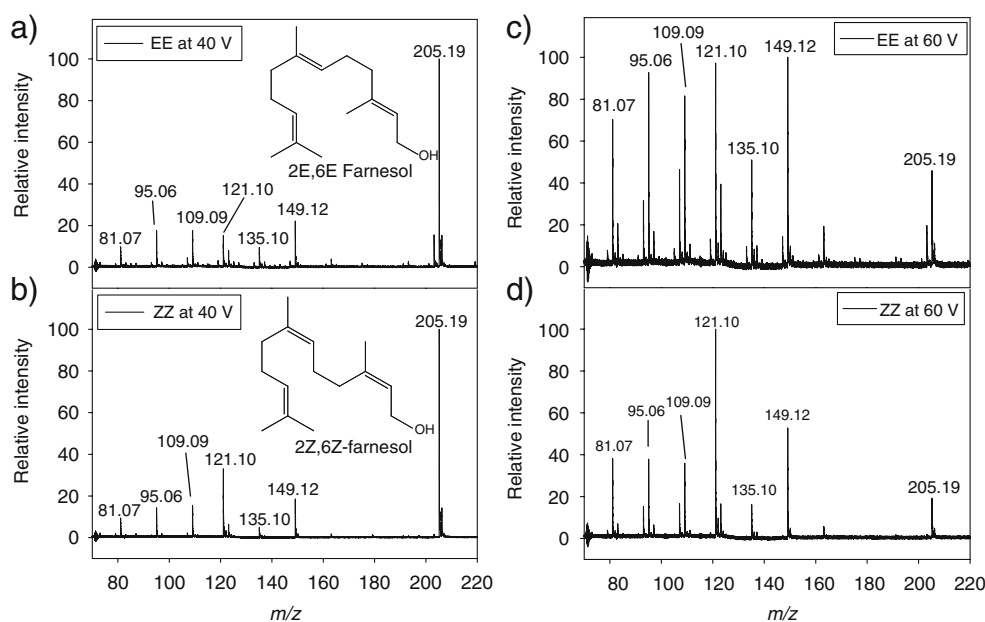
Limit of detections of the optimized DART-oaTOF MS method

Figure 3 shows DART-oaTOF mass spectra obtained from a 0.1 pmol/μL solution of (2E,6E)-farnesol (Fig. 3a), 4 pmol/μL of both, FA (Fig. 3b) and MF (Fig. 3c), and 1 pmol/μL solution of JH III (Fig. 3d). Mass spectra of all analytes showed base peaks corresponding to protonated [M+H]$^+$ ions, except for farnesol, in which with the water loss ion was the dominant peak. The experimentally observed mass accuracies for the analytes were as follows: 0.6 ppm for [farnesol–H$_2$O+H]$^+$ (m/z 205.1952), 5.8 ppm for [FA+H]$^+$ (m/z 273.1863), 1.8 ppm for [MF+H]$^+$ (m/z 251.2001), and 0.8 ppm for [JH III+H]$^+$ (m/z 267.1957). The experimentally calculated signal-to-noise (S/N) ratios for these analytes were 12 for farnesol (0.1 pmol/μL), 16.5 for FA (4 pmol/μL), 18.4 for MF (4 pmol/μL), and 24.4 for JH III (1 pmol/μL), as shown in Fig. 3a–d. The detection limits calculated from these S/N ratios were as follows: 25 fmol/μL for farnesol, 730 fmol/μL for FA, 650 fmol/μL for MF, and 123 fmol/μL for JH III. These are the 'absolute best' achievable detection values and are expected to be higher for a real world sample due to the presence of interfering sample matrix and buffers. The higher ionization efficiency of JH III compared to FA and MF can be rationalized based on the corresponding molecular structures. Unlike FA and MF, JH III contains an epoxy group that can serve as an additional proton binding site, contributing to a higher basicity of this molecule.

Reported levels of JH in hemolymph or insect whole body extracts vary between 20 and 4500 pg/μl [12, 14], and levels of JH biosynthesis by isolated CA fluctuate between 110 fmol and 50 pmol per CA/h [11, 13]. Therefore, the sensitivity afforded by the optimized DART-oaTOF method is expected to allow for the detection of terpenes from insect extracts *or corpora allata* cultured in vitro, with a sample throughput of three samples per minute. As compared to the established analytical methods such as HPLC-MS and GC-MS, the proposed DART-MS method offers a much shorter analysis time of few minutes, and requires less that 5 μL of sample volume. Previously reported detection limits of JH using HPLC-MS [39] are comparable to those obtained using DART-MS, emphasizing the potential of this technique in analyzing low levels of terpenes with shorter turn-around times. Additionally, since minimal fragmentation is observed in DART-MS, as compared to GC-MS, maximum sensitivity can be achieved by observing the precursor ion instead of its fragments [40]. However, further developments in DART sampling techniques are still needed in order to use DART-MS for accurate quantitative analysis with acceptable reproducibility and repeatability, usually achievable by the conventional methods.

Distinguishing between farnesol isomers by DART in-source CID oaTOF MS

In addition to accurate mass measurements, in-source CID can also produce useful information for structural determination purposes. Along this line of thought, DART in combination with CID experiments was used for distinguishing between two farnesol isomers. Studies of enzymatic oxidation of farnesol in some insects such as *Manduca sexta* have showed high specificity for one particular isomer [8]. Furthermore, only one farnesol stereoisomer has biological activity in nutria [19]. Therefore, distinguishing between active and inactive isomers is important from the biological point of view. The fragmen-
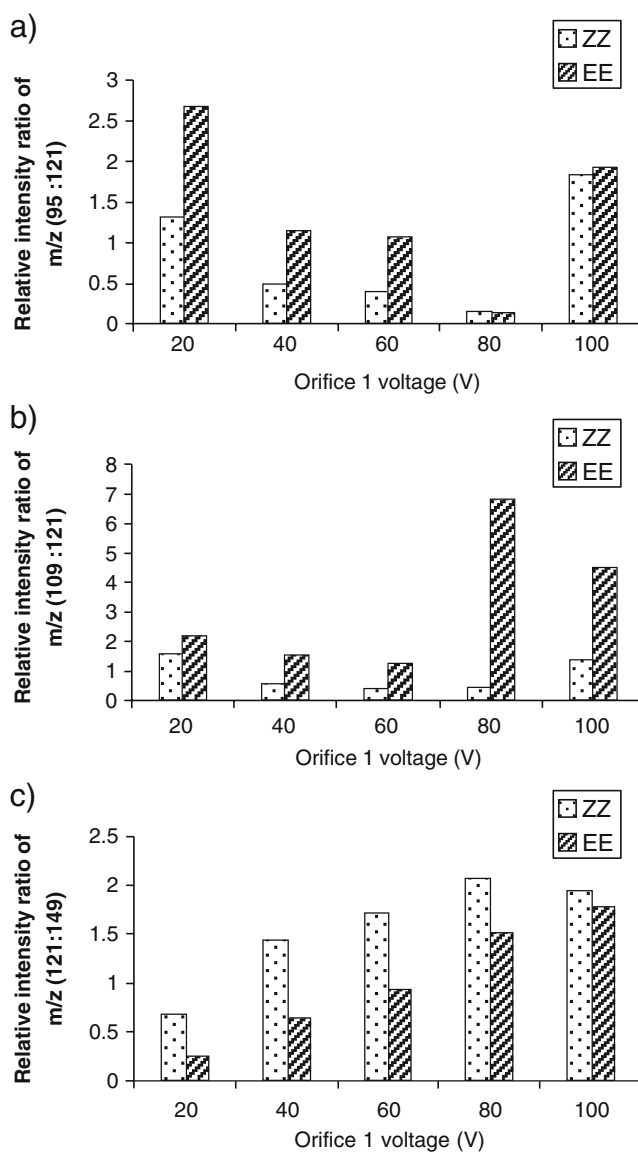
Fig. 5 Relative intensity ratios for various pairs of fragment ions **a** 95:121, **b** 109:121, and **c** 121:149 as a function of orifice 1 voltage for (2Z,6Z)- and (2E,6E)-farnesol

tation profiles of farnesol isomers obtained by CID MS could serve as fingerprints for identifying the stereochemistry of endogenous farnesol in insects. Similar studies undertaken by Lee et al. [19] to determine the configurations of four farnesol isomers using EI and CI were only partially successful as the CI mass spectra of the isomers only showed small differences in fragmentation patterns. To that end, we explored in-source CID DART as an alternative strategy for selective stereoisomer discrimination.

Working solutions of both farnesol isomers were subjected to in-source CID at various orifice 1 voltages. The 40 V in-source CID mass spectra of both isomers showed common fragments at m/z 81, 95, 109, 121, 135, and 149, along with the base peak at m/z 205.19, arising from neutral loss of one water molecule from the protonated farnesol ion (Fig. 4a–b). When compared against the corresponding NIST EI MS reference database, DART-oaTOF CID spectrum of farnesol showed some similarities in its spectral features to the corresponding database entry [41]. EI mass spectra of most aliphatic alcohols show alkene ions arising from water losses as the dominant species. Therefore, it has been suggested that these alkene ions rather than their alkanols be considered as the origin for most EI fragment ions [42]. The EI mass spectra of aliphatic alkenes show loss of neutral ethene ($-C_nH_{2n}$) units [43]. A similar fragmentation pathway explains the observed farnesol CID fragment ions (Fig. 4). After the protonated farnesol alkene is formed by water loss, it undergoes further fragmentation by losses of various ethene units. The fragment ions thus formed were as follows: m/z 163.15 ($-C_3H_6$), 149.13 ($-C_4H_8$), 135.11 ($-C_5H_{10}$), 121.10 ($-C_6H_{12}$), 107.08 ($-C_7H_{14}$), and m/z 93.06 ($-C_8H_{16}$). Further investigation, by deuterium labeling studies should be pursued to support the previous hypothesis.

As the acceleration voltage was increased from 40 to 60 V, intense fragment ion signals dominated the CID spectra of both isomers (Fig. 4c–d). Breakdown plots were obtained to study the differences in the fragmentation profiles of some of the commonly observed fragments in respective CID mass spectra (Figure S3, ESM). Overall, the relative fragmentation efficiency of the EE-isomer was found to be greater than that of ZZ-farnesol at orifice 1 voltages between 40 and 80 V. From these breakdown plots, the relative intensity ratios of several fragment ions at various orifice 1 voltages were investigated (Fig. 5a–c). It was observed that the relative intensity ratios of fragments 95:121 (Fig. 5a) and 121:149 (Fig. 5c) were appreciably different for the two isomers at all orifice 1 voltages, except for 80 and 100 V. On the other hand, dramatic differences in the ratio of 109:121 were observed in this collision energy range (Fig. 5b). These variations correlate with the different configurations of carbon–carbon double bond at C-2 of the two farnesol isomers. The encouraging results

from these experiments highlighted the potential of using in-source CID of DART ions for stereoisomer discrimination.

Conclusion

An in-depth characterization and optimization of DART parameters allowed for the development of a high-sensitivity DART-oaTOF MS approach for the rapid analysis of insect terpenoids. The examination of DART-oaTOF mass spectra of farnesol revealed the presence of a molecular ion along with the corresponding protonated species, indicating the presence of competing ionization mechanisms. With the optimized DART-MS method, detection limits ranging from femtomole to sub-picomole were achieved for JH III and its precursors. With such detection limits and mass accuracies below 5 ppm, it could be possible to selectively detect endogenous levels of these biologically active molecules. Additionally, we have shown that in principle it is possible to distinguish between farnesol isomers based on differences in the in-source CID fragmentation profiles.

References

1. Goodman W, Granger N (2005) in:Iatrou, K., Gilbert, L., and Gill S (ed) Comprehensive Molecular Insect Science, 1st Edn., Elsevier, Oxford
2. Wilson TG (2004) J Insect Physiol 50:111–121
3. Dhadialla TS, Carlson GR, Le DP (1998) Annu Rev Entomol 43:545–569
4. Lococo DJ, Tobe SS (1984) Int J Insect Morphol Embryol 13:65–76
5. Belles X, Martin D, Piulachs MD (2005) Annu Rev Entomol 50:181–199
6. Cao L, Zhang P, Grant DF (2009) Biochem Biophys Res Commun 380:188–192
7. Mayoral JG, Nouzova M, Navare A, Noriega FG (2009) Proc Natl Acad Sci U S A
8. Baker FC, Mauchamp B, Tsai LW, Schooley DA (1983) J Lipid Res 24:1586–1594
9. Mayoral JG, Nouzova M, Yoshiyama M, Shinoda T, Hernandez-Martinez S, Dolghih E, Turjanski AG, Roitberg AE, Priestap H, Perez M, Mackenzie L, Li Y, Noriega FG (2009) Insect Biochem Mol Biol 39:31–37
10. Helvig C, Koener JF, Unnithan GC, Feyereisen R (2004) Proc Natl Acad Sci USA 101:4024–4029
11. Bloch G, Borst DW, Huang Z, Robinson GE, Cnaani J, Hefetz A (2000) J Insect Physiol 46:47–57
12. Shapiro A, Wheelock G, Hagedorn H, Baker F, Tsait L, Schooley D (1986) J Insect Physiol 32:867–877

13. Taub-Montemayor TE, Min KJ, Chen Z, Bartlett T, Rankin MA (2005) J Insect Physiol 51:427–434
14. Trumbo ST, Robinson GE (2008) J Insect Physiol 54:630–635
15. Mayoral JG, Nouzova M, Yoshiyama M, Shinod T, Hernandez-Martinez S, Dolghih E, Turjanski AG, Roitberg AE, Priestap H, Perez M, Mackenzie L, Li YP, Noriega FG (2009) Insect Biochem Mol Biol 39:31–37
16. Li Y, Unnithan GC, Veenstra JA, Feyereisen R, Noriega FG (2003) J Exp Biol 206:1825–1832
17. Teal PE, Proveaux AT, Heath RR (2000) Anal Biochem 277:206–213
18. Bergot BJ, Ratcliff M, Schooley DA (1981) J Chromatogr 204:231–244
19. Lee H, Finckbeiner S, Yu JS, Wiemer DF, Eisner T, Attygalle AB (2007) J Chromatogr A 1165:136–143
20. Cody RB, Laramee JA, Durst HD (2005) Anal Chem 77:2297–2302
21. Fernandez FM, Hampton CY, Nyadong L, Navare A, Kwasnik M (2009) In LC/TOF-MS for accurate mass analysis: principles, tools, and applications for accurate mass analysis. Ferrer I, Thurman EM (eds), Wiley Hoboken, NJ
22. Penning FM (1927) Naturwissenschaften 15:818–818
23. Jones RW, Cody RB, McClelland JF (2006) J Forensic Sci 51:915–918
24. Petucci C, Diffendal J, Kaufman D, Mekonnen B, Terefenko G, Musselman B (2007) Anal Chem 79:5064–5070
25. Fernandez FM, Cody RB, Green MD, Hampton CY, McGready R, Sengaloundeth S, White NJ, Newton PN (2006) ChemMedChem 1:702–705
26. Newton PN, Fernandez FM, Plancon A, Mildenhall DC, Green MD, Ziyong L, Christophel EM, Phanouvong S, Howells S, McIntosh E, Laurin P, Blum N, Hampton CY, Faure K, Nyadong L, Soong CW, Santoso B, Zhiguang W, Newton J, Palmer K (2008) PLoS Med 5:e32
27. Newton PN, McGready R, Fernandez F, Green MD, Sunjio M, Bruneton C, Phanouvong S, Millet P, Whitty CJ, Talisuna AO, Proux S, Christophel EM, Malenga G, Singhasivanon P, Bojang K, Kaur H, Palmer K, Day NP, Greenwood BM, Nosten F, White NJ (2006) PLoS Med 3:e197
28. Vail T, Jones PR, Sparkman OD (2007) J Anal Toxicol 31:304–312
29. Rothenbacher T, Schwack W (2009) Rapid Commun Mass Spectrom 23:2829–2835
30. Haefliger OP, Jeckelmann N (2007) Rapid Commun Mass Spectrom 21:1361–1366
31. Pierce CY, Barr JR, Cody RB, Massung RF, Woolfitt AR, Moura H, Thompson HA, Fernandez FM (2007) Chem Commun (Camb) 807-9
32. Yu S, Crawford E, Tice J, Musselman B, Wu JT (2009) Anal Chem 81:193–202
33. Zhou M, McDonald JF, Fernandez FM (2009) J Am Soc Mass Spectrom 21:68–75
34. Harris GA, Fernandez FM (2009) Anal Chem 81:322–329
35. Keniti H, Nozoe T, Omura I (1957) BCSJ 30:408–410
36. Kazakov SM, Kaputerko MN, Suchkov VA (1999) J Appl Spectrosc 66:375–379
37. Hanebeck W, Gasteiger J (1993) J Comput Chem 14:138–154
38. Cody RB (2009) Anal Chem 81:1101–1107
39. Westerlund SA, Hoffmann KH (2004) Anal Bioanal Chem 379:540–543
40. Teal PEA, Proveaux AT, Heath RR (2000) Anal Biochem 277:206–213
41. http://webbook.nist.gov/cgi/cbook.cgi?Name=farnesol&Units=SI&cMS=on
42. Gross JH (2004) Mass spectrometry: a textbook. Springer, Berlin
43. Carroll DI, Dzidic I, Stillwell RN, Haegele KD, Horning EC (1975) Anal Chem 47:2369–2373